

Cytotoxic Therapy-Induced Effects on Both Hematopoietic and Marrow Stromal Cells Promotes Therapy-Related Myeloid Neoplasms

Angela Stoddart¹, Jianghong Wang¹, Anthony A. Fernald¹, Elizabeth M. Davis¹, Camille R. Johnson¹, Chunmei Hu¹, Jason X. Cheng^{2,3}, Megan E. McNerney^{2,3,4}, and Michelle M. Le Beau^{1,3}

ABSTRACT

Therapy-related myeloid neoplasms (t-MN) following treatment with alkylating agents are characterized by a del(5q), complex karyotypes, alterations of *TP53*, and a dismal prognosis. To decipher the molecular pathway(s) leading to the pathogenesis of del(5q) t-MN and the effect(s) of cytotoxic therapy on the marrow microenvironment, we developed a mouse model with loss of two key del(5q) genes, *EGR1* and *APC*, in hematopoietic cells. We used the well-characterized drug, N-ethyl-N-nitrosourea (ENU), to demonstrate that alkylating agent exposure of stromal cells in the microenvironment increases the incidence of myeloid disease. In addition, loss of *Trp53* with *Egr1* and *Apc* was required to drive the development of a transplantable leukemia, and accompanied by the acquisition of somatic mutations in DNA damage response genes. ENU treatment of mesenchymal stromal cells induced cellular senescence and led to the acquisition of a senescence-associated secretory phenotype, which may be a critical microenvironmental alteration in the pathogenesis of myeloid neoplasms.

SIGNIFICANCE: This study challenges the historic view that prior cytotoxic therapy targets only hematopoietic cells and shows that chemotherapy-induced alterations to the microenvironment contribute to myeloid neoplasms in a model of del(5q) t-MN. The DNA damage response in hematopoietic cells and senescence of stromal cells are identified as potential therapeutic targets.

INTRODUCTION

Therapy-related myeloid neoplasms (t-MN) comprise therapy-related acute myeloid leukemia (t-AML) and myelodysplastic syndrome (t-MDS), and are a late complication of cytotoxic therapy, chemotherapy and/or radiotherapy, used in the treatment of both malignant and nonmalignant diseases (1, 2). The genetic profile of t-MN is markedly skewed toward high-risk cytogenetic and molecular abnormalities, and complex karyotypes with deletions of the long arm of chromosome 5, del(5q), and *TP53* mutation/loss are profoundly over-represented in t-MNs as compared with *de novo* counterparts (3, 4). A proximal minimally deleted region (MDR) in 5q31.2 (containing *EGR1*) was previously identified in t-MN, *de novo* AML and high-risk MDS, and a distal MDR in 5q33.1 (containing *mir145*, *RPS14*, and *CSNK1A1*) was identified in MDS with an isolated del(5q), previously referred to as the 5q- syndrome (1, 5). However, the deletion of 5q in all but rare patients encompasses both MDRs, spanning 5q14-5q33, resulting in loss of one allele for hundreds of genes. Although challenging to identify involved genes, we previously chose to examine two well-characterized del(5q)

tumor suppressor genes, early growth response 1 (*EGR1*; 5q31.2) and adenomatous polyposis coli (*APC*; 5q22.2), and showed that they cooperate with *TP53* (*p53*) loss to induce acute myeloid leukemia in mice (6). The low frequency of AML and long latency observed in this model, however, suggests that additional stochastic events, and/or mutations arising from environmental exposures, may contribute to the etiology of disease.

Healthy individuals harbor clonal, somatic, gene mutations in white blood cells, and the frequency increases with age, leading to the expansion of some clones, a phenomenon known as “clonal hematopoiesis of indeterminate potential,” (CHIP) (CHIP; refs. 7, 8). Recent studies have revealed that CHIP increases the risk for t-MN (9, 10). The landmark finding of preexisting *TP53* mutations in hematopoietic cells originating prior to cytotoxic treatment of a primary malignant disease and in the t-MNs that subsequently evolved, led to the proposal that chemotherapy and/or radiation may preferentially impair normal hematopoietic stem and progenitor cells (HSPC), while providing a selective advantage to clones with preexisting mutations (11). Follow-up studies showed that cytotoxic therapy results in the expansion of clones carrying mutations in DNA damage response genes, including *TP53*, *PPM1D*, *ATM*, *BRCC3*, *SRCAP*, and *RAD21* (12); however, mutations in DNA repair genes, other than *TP53* and *PPM1D* (11–13), are not present in leukemia samples isolated from patients with t-MN. Interestingly, the DNA double-strand break response is abnormal in myeloblasts from t-MNs, even though somatic mutations of DNA repair genes do not appear to be the dominant mechanism responsible for this phenotype (14).

In addition to alterations in hematopoietic cells, there is compelling data suggesting that alterations to the bone marrow microenvironment also play a role in the pathogenesis of myeloid neoplasms (15–18). These alterations may include establishment of an inflammatory microenvironment (19)

¹Department of Medicine, The University of Chicago, Chicago, Illinois.

²Department of Pathology, The University of Chicago, Chicago, Illinois. ³The University of Chicago Medicine Comprehensive Cancer Center, Chicago, Illinois. ⁴Department of Pediatrics, The University of Chicago, Chicago, Illinois.

Note: Supplementary data for this article are available at Blood Cancer Discovery Online (<http://cancerdiscovery.aacrjournals.org/>).

Corresponding Author: Angela Stoddart, The University of Chicago, 900 E. 57th Street, Office Room 7122, Lab 7240, Chicago, IL 60637. Phone: 773-702-9164; Fax: 773-702-9268; E-mail: astoddar@bsd.uchicago.edu
Blood Cancer Discov 2020;1–16

doi: 10.1158/2643-3230.BCD-19-0028

©2020 American Association for Cancer Research.

and/or age-associated changes of mesenchymal stromal cells (MSC; ref. 20). MSCs isolated from patients with MDS and AML display several characteristic features of senescence, including TP53 pathway activation (21, 22), increased senescence-associated β -galactosidase (SA- β -gal) expression (22–24), and upregulation of senescence-associated secretory phenotype (SASP) factors, such as IL6 (25, 26). Moreover, AMLs can induce a senescent phenotype in bone marrow (BM) stromal cells, and targeting these senescent cells improves the survival of mice with leukemia (25), illustrating the importance of a senescent microenvironment in the pathophysiology of leukemia.

The complete compendium of genetic alterations and selective pressures leading to t-MN with a del(5q) remain unknown, especially with regard to the effects of cytotoxic therapy on the microenvironment. In this study, we use a multifaceted approach to model del(5q) t-MN in mice, and to define genetic alterations in HSPCs by whole exome and RNA sequencing, while simultaneously probing hematopoietic stem cell (HSC)-intrinsic and cell-extrinsic effects of alkylating-agent therapy. Our results pinpoint chemotherapy-induced alterations to BM stromal cells and genetic alterations to DNA repair genes in HSPCs as two factors critical for the pathogenesis of del(5q) t-MNs with aberrant TP53.

RESULTS

Alkylating Agent Exposure Increases the Incidence of Myeloid Disease

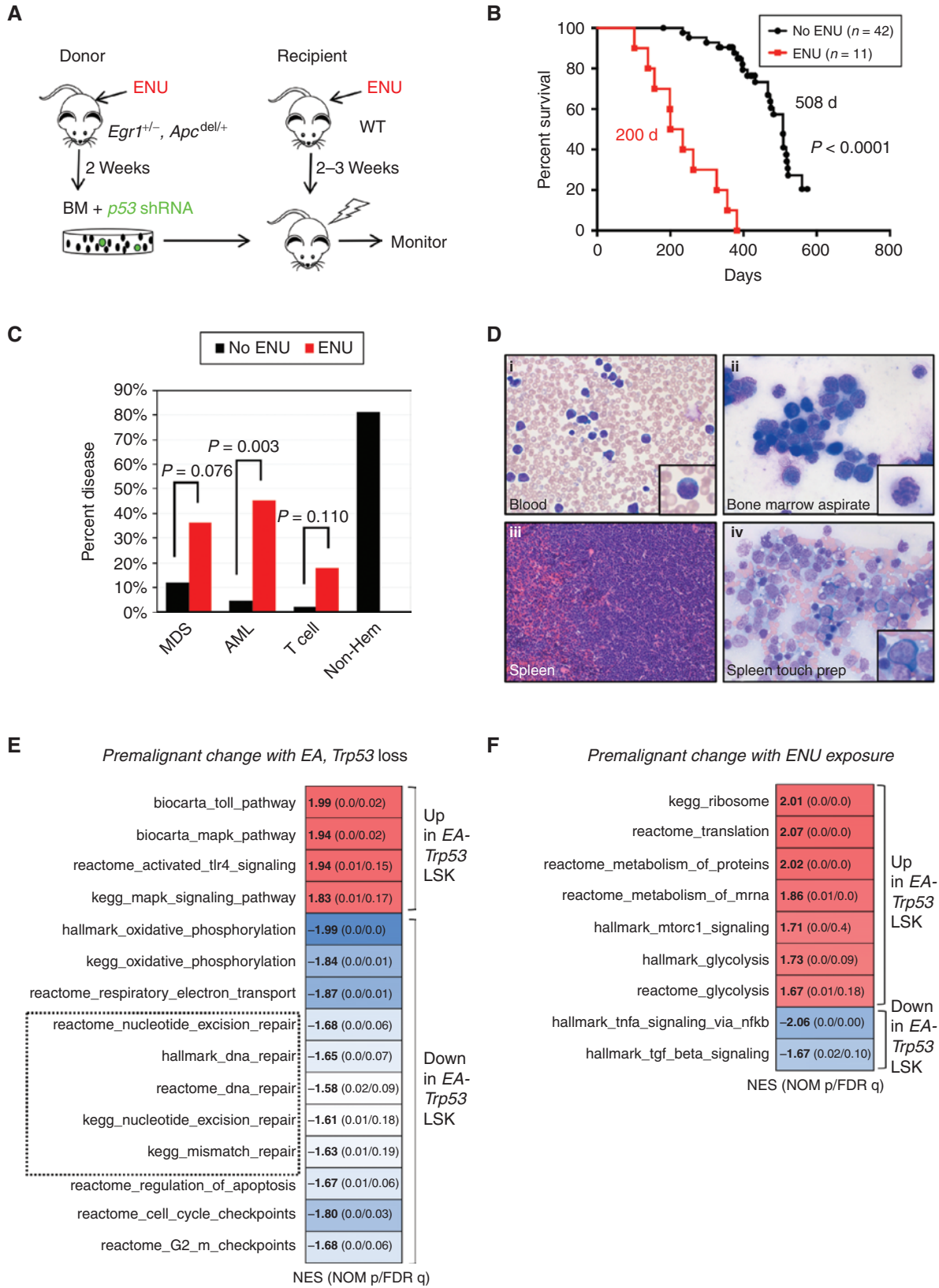
A striking 40% of patients with t-MN have a del(5q) (2), the majority (>95%) of which have haploinsufficient loss of both *EGR1* (27) and *APC* (28). Moreover, approximately 75% of del(5q)t-MNs have loss and/or mutation of the *TP53* gene (29). To model this, we previously showed that cell-intrinsic loss of both *Egr1* and *Apc*, or individual loss of either *Egr1* or *Apc*, together with *Trp53* knock-down, was not sufficient to promote AML; however, concordant loss of the three genes, *Egr1*, *Apc*, and *Trp53*, modeled the development of del(5q) AML (ref. 6; Supplementary Fig. S1). In clinical settings, however, patients with t-MN receiving chemotherapy have expo-

sure of the entire body, including the BM microenvironment and HSPCs. The relative contribution of drug treatment on the niche and/or HSPCs, and the interplay of genetics, the microenvironment, and chemotherapy, in subsequent t-MN development is unclear.

To isolate these variables, we employed our del(5q) mouse model, with *Egr1* and *Apc* haploinsufficiency and loss of *Trp53*, which spontaneously develops leukemia at a low frequency (<20%; ref. 6). However, in this study, we treated HSPCs and the niche separately with N-ethyl-N-nitrosourea (ENU), a prototypical alkylating agent whose effects have been well characterized in mice. We first assessed the outcome of ENU exposure of both the niche and hematopoietic cells. *Egr1*^{+/-}, *Apc*^{del/+} donor and wild-type (WT) recipient mice were treated with ENU. *Egr1*^{+/-}, *Apc*^{del/+} BM cells were isolated two weeks after ENU treatment, transduced with *Trp53* shRNA to knock-down expression of *Trp53* (*Trp53* KD), and transplanted into ENU-treated, lethally irradiated WT recipient mice (Fig. 1A).

Compared with donor and recipient mice that did not receive ENU (no ENU), alkylating agent exposure significantly accelerated the onset of disease with a median survival of 200 days versus 508 days ($P < 0.0001$; Fig. 1B). In accordance with the Bethesda classification (30), the disease was classified as a myeloid leukemia when at least 20% blasts were observed in hematopoietic tissue, and as a MDS when anemia and morphologic dyspoiesis was observed. A significantly larger percentage of mice developed MDS (36% vs. 12%, $P = 0.076$) or AML (45% vs. 5%, $P = 0.003$) in the ENU-treated group as compared with untreated mice (Fig. 1C). Eighty percent of non-ENU-treated mice did not develop hematologic disease (non-Hem) and were sacrificed due to age and poor health. The myeloid malignancies that developed in ENU-treated mice resembled human disease ranging from MDS-refractory anemia with excess blasts-1 or -2 (RAEB-1 or -2) to AML with myelodysplasia-related changes (Fig. 1D; Supplementary Fig. S2A). Mice with myeloid neoplasms presented with splenomegaly and an effacement of the normal splenic architecture, as well as trilineage dysplasia similar to that observed in patients with t-MN with a del(5q) (Supplementary Figs. S2B and S3). Disease in mice with blast counts >20%, and classified as AML, was transplantable to secondary

Figure 1. Alkylating agent therapy increases the incidence of myeloid neoplasms. **A**, Schematic of ENU treatment and transplantation scheme used to develop a mouse model of t-MN. *Egr1*^{+/-}, *Apc*^{del/+} BM cells were transduced with *Trp53* shRNA, and transplanted into lethally irradiated WT recipient mice. For the ENU cohort, donor mice were treated once with 100 mg/kg ENU 2 weeks before BM harvest; recipients were treated once with 100 mg/kg ENU, 2 to 3 weeks before lethal irradiation and transplantation. **B**, Kaplan–Meier survival curves of untreated and ENU-treated mice. Percentage survival (time to sacrifice) is plotted versus time in days. In the absence of ENU treatment, the mice survive significantly longer (508 days vs. 200 days, $P < 0.001$), with a small percentage developing MDS/AML, but the majority succumb to advanced age and nonhematologic effects. **C**, Histologic classification of diseases that arose in the no-ENU and ENU-treated mice. There is a significantly increased frequency of AML in the ENU-treated group. Most of the no-ENU mice died due to age-related issues rather than hematopoietic malignancies. Disease frequency was compared using Fisher exact test. **D**, Images of the myeloid disease in ENU-treated mice were obtained using an Olympus BX41 microscope and a 50 \times /0.9 (oil) or 40 \times /0.9 objective, and processed with Adobe Photoshop. Peripheral blood smears, BM smears, and spleen touch preparations were stained with Wright–Giemsa (500 \times magnification), and spleen sections were stained with hematoxylin and eosin (200 \times magnification). Examples of a myeloblast (inset i), dysplastic granulocyte (inset ii), sheets of infiltrating blasts (inset iii), and a dysplastic erythroid precursor (inset iv) are shown. **E** and **F**, LSK⁺ (Lin⁻, Sca1⁺, Kit⁺) cells were sorted from three different mouse cohorts: recipients of WT, luc shRNA⁺ BM (controls; $n = 3$), recipients of *Egr1*^{+/-}, *Apc*^{del/+}, *Trp53* shRNA⁺ cells (EA-*Trp53*), either untreated ($n = 3$) or treated with ENU ($n = 3$), approximately 70 to 90 days after transplant, prior to the onset of overt leukemia. **E**, GSEA of WT control ($n = 3$) compared with EA-*Trp53* LSK⁺ samples [includes both the no-ENU and ENU-treated groups ($n = 6$)] to identify premalignant changes as a consequence of *Egr1*, *Apc*, and *Trp53* loss. **F**, GSEA of EA-*Trp53* LSK⁺ samples from the no-ENU ($n = 3$) versus ENU-treated ($n = 3$) group was used to identify genetic consequences of *in vivo* ENU exposure. Biological pathways/processes that were significantly enriched (FDR < 20%, nominal $P < 0.05$) in two or more Molecular Signatures Database (MSigDB) gene sets are shown. Heatmap of the normalized enrichment scores (NES) shows that DDR pathways (DNA repair, apoptosis, checkpoints) are downregulated due to loss of *Egr1*, *Apc*, and *Trp53*, with or without ENU treatment. **E**, Energy production pathways, such as mTORC1, protein translation, and glycolysis, are upregulated as a consequence of ENU exposure (**F**).



recipients and was, thus, no longer dependent on an ENU-exposed niche (Supplementary Table S1).

To decipher the molecular pathways that are altered in the premalignant state, we sorted *Egr1*^{+/−}, *Apc*^{del/+}, GFP⁺, *Trp53*-deficient lineage[−], Sca-1⁺, Kit⁺ progenitors (*EA-Trp53* LSKs) from both the no-ENU (*n* = 3) and ENU-treated (*n* = 3) groups prior to the development of overt leukemia (~80 days posttransplant) and performed RNA sequencing (RNA-seq). As a control, three independent LSK⁺ samples were obtained from WT recipients of WT BM transduced with a nonspecific (luciferase) shRNA. To decipher the effects of *EA-Trp53* loss, we compared WT control (*n* = 3) with *EA-Trp53* LSK⁺ samples [includes both the no-ENU and ENU-treated groups; (*n* = 6); Fig. 1E]. Gene set enrichment analysis (GSEA; ref. 31) of the top enriched curated pathways revealed that cell-intrinsic loss of *Egr1*, *Apc*, and *Trp53* downregulates oxidative phosphorylation, DNA repair, apoptosis, and cell-cycle checkpoints. Similar results were observed when we compared only the three ENU-exposed *EA-Trp53* LSK⁺ samples with WT controls (Supplementary Fig. S4).

To elucidate the effects of ENU, we compared *EA-Trp53* cells with and without ENU exposure (Fig. 1F). ENU exposure increased the expression of genes involved in energy production, such as mTOR signaling and protein translation (Fig. 1F); however, we cannot rule out that this simply reflects cells that are at a more advanced stage along the continuum of malignant transformation with higher metabolic activity, rather than a direct effect of ENU exposure. Interestingly, similar changes in gene expression were observed in patients who subsequently developed t-MN (32). Together, these results are consistent with a role for loss of genome defense mechanisms in the development of myeloid neoplasms.

Incidence of AML Increases When *Egr1*, *Apc*, and *Trp53*-deficient HSPCs as well as the BM Microenvironment Are Exposed to Cytotoxic Therapy

We next separately tested the effects of alkylating agent therapy on HSPCs or the BM microenvironment. To test the effect on HSPCs, we treated only BM donors with ENU (2 weeks prior to BM isolation for *Trp53* knockdown, Fig. 2A). To test the impact on the niche, we treated transplant recipients only (2–3 weeks prior to transplant).

Approximately 10% of *Egr1*^{+/−}, *Apc*^{del/+} BM cells were transduced with the GFP-positive *Trp53* shRNA (*Trp53* shRNA-GFP⁺) prior to transplantation (Fig. 2B, % GFP⁺, black circles). This relatively low frequency allowed us to assess the effect of ENU on the competitive expansion of *Trp53*-deficient, *Egr1*^{+/−}, *Apc*^{del/+} BM cells. ENU treatment of recipient or donor mice led to a modest expansion of *Trp53* shRNA-GFP⁺ cells 1.5 to 5 months after transplant. However, the greatest expansion of *Trp53* shRNA-GFP⁺ cells was observed when both donor and recipients were treated with ENU, suggesting that ENU exposure of both HSPCs and the microenvironment contributes to clonal expansion.

Even though ENU treatment of donor or recipient mice increased the expansion of *Trp53* shRNA-GFP⁺ cells, it did not accelerate disease development (Fig. 2C; 517 days or 533 days vs. 508 days without ENU treatment), nor did it increase the frequency of myeloid neoplasms beyond what is

observed without ENU treatment (Fig. 2D; compare “none” to “donor” or “recipient”). Only 1 of 10 recipient-treated mice developed AML, and none of the donor-treated mice developed a myeloid neoplasm [two died early from T lymphomas; the remainder were sacrificed (>500 days) due to age-related causes]. In contrast, 82% of mice, in which both donor and recipient mice were exposed to ENU, developed MDS or AML. Thus, whereas exposure of HSPCs or the microenvironment alone to ENU promotes expansion of *Trp53*-shRNA⁺ cells, t-MN development is driven by the synergistic effects of chemotherapy exposure of premalignant hematopoietic cells, together with deleterious effects of cytotoxic therapy on the supporting microenvironment. Historically, it has been assumed that the effect of prior therapy in patients who develop t-MN was primarily on the HSPCs. To our knowledge, this is the first mouse model of del(5q) t-MN to directly show that chemotherapy-induced alterations to the BM microenvironment contribute to disease development.

Alkylating Agent Exposure Induces Senescence of Mesenchymal Stromal Cells

In solid tumors, there is evidence that senescence of non-tumor cells promotes tumor growth and metastasis (33). Furthermore, cytotoxic treatment induces an acute inflammatory response in the BM microenvironment. We hypothesized that ENU induces a sustained effect via senescence of MSCs within the microenvironment and, thereby, alters the function of HSPCs. To evaluate this hypothesis, MSCs were treated for 24 hours with increasing doses of ENU, and senescence was assessed 7 days later. MSCs treated with ENU showed an increase in SA-β-gal activity and a decline in DNA synthesis as determined by EdU incorporation (Fig. 3A and B). Senescence was further confirmed by elevated levels of mRNA encoding p21 (Cdkn1a), p16INK4a (Cdkn2a), and IL6 (Fig. 3C).

We next examined MSCs isolated from mice treated with one dose of ENU, which showed a decreased number of colony-forming unit-fibroblasts (CFU-F; Fig. 3D and E) and an increase in SA-β-gal activity (Fig. 3F). Consistent with the finding that damage-initiated senescence strongly depends on *TP53* (34), GSEA analysis of RNA-seq data revealed activation of the p53 pathway in MSCs isolated from ENU-treated mice, compared with mock-treated mice (Fig. 3G). Senescent cells express and secrete a variety of extracellular modulators collectively referred to as the senescence-associated secretory phenotype (SASP; ref. 35). Enrichment of a SASP GSEA signature was observed in MSCs isolated from ENU-treated mice (Fig. 3H), providing a potential mechanism by which they contribute to the pathogenesis of leukemia.

To assess whether an ENU-treated microenvironment affects stem cell fitness *in vivo*, a competitive BM transplant assay was performed as outlined in Fig. 3I. We used *Egr1*^{+/−} donor cells, because *Egr1* has been documented to play a role in stem cell quiescence (36). The repopulation ratio of CD45.2⁺ (*Egr1*^{+/+}) to CD45.1⁺ short-term-HSC (ST-HSC) cells was normalized to 100% (mock conditions). In mock conditions, *Egr1*^{+/−} ST-HSCs displayed a reduced normalized repopulation ratio of 31%. Although not statistically different (*P* = 0.31), this trend may reflect stem cell exhaustion due to *Egr1*'s role in maintaining stem cell quiescence. With ENU treatment (red bars), *Egr1*^{+/−} ST-HSCs showed

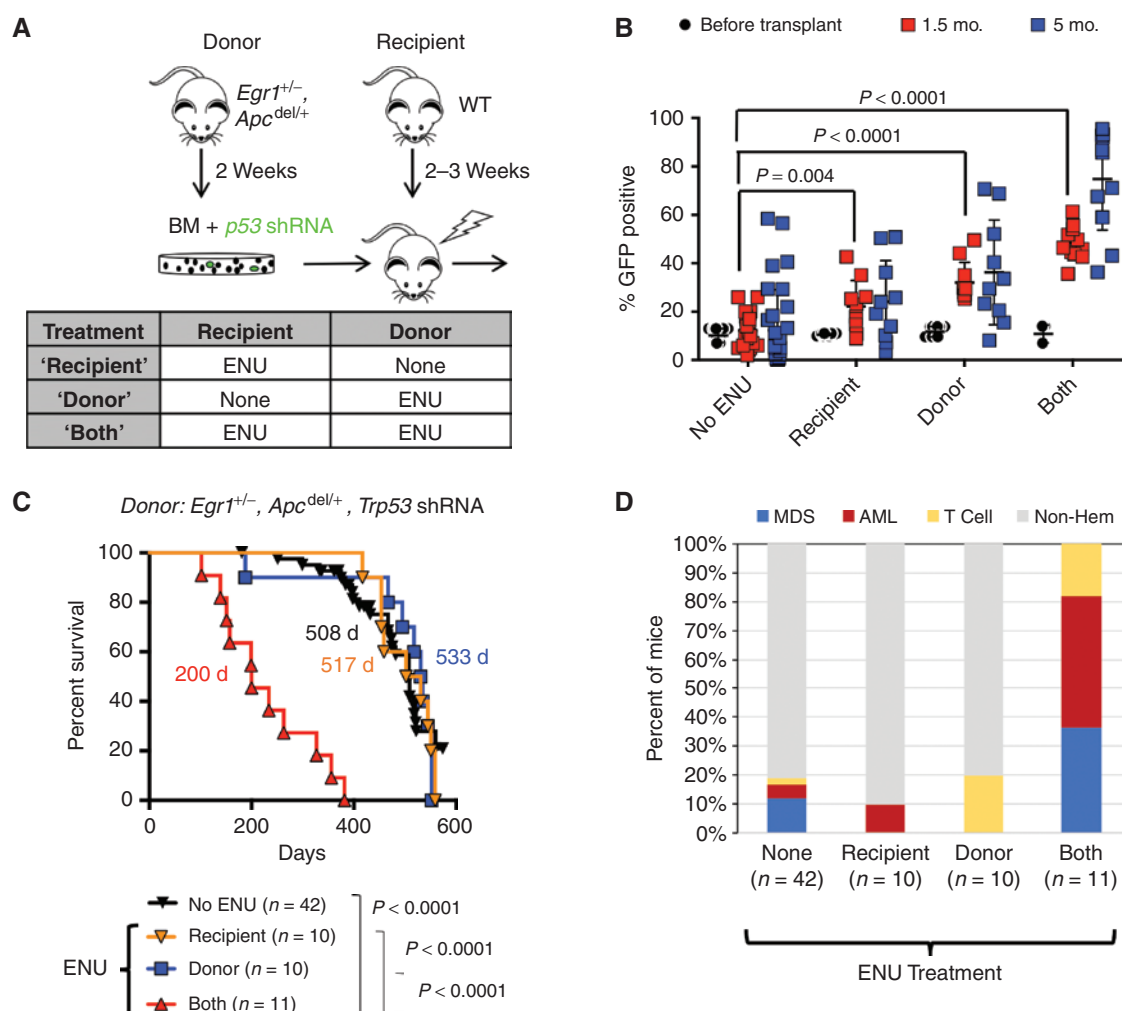


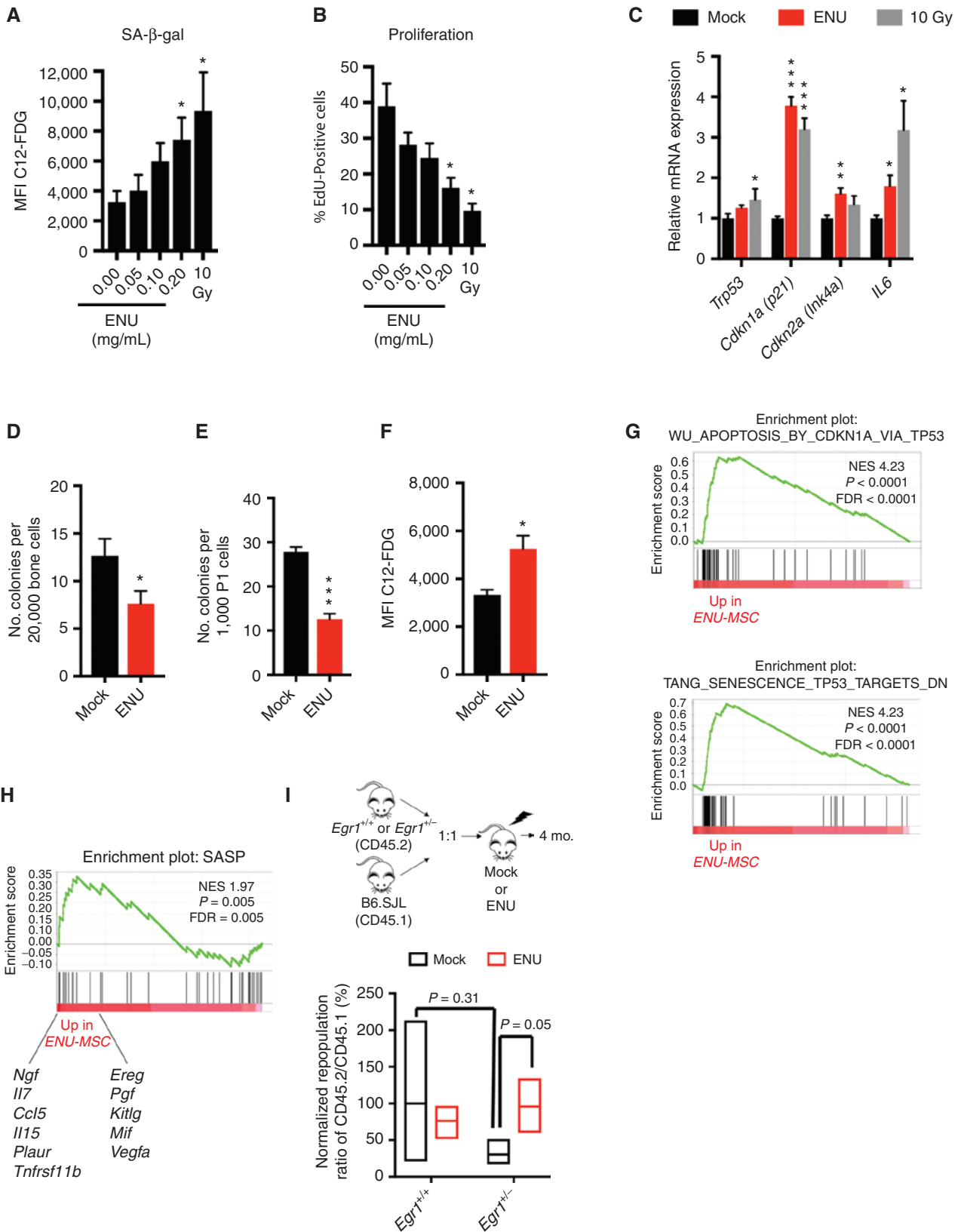
Figure 2. Exposure of the BM microenvironment to ENU plays a critical role in the development of MDS and AML. **A**, Schematic of the transplantation schemes used to elucidate the effects of alkylating agents on HSPCs, with *Trp53* knockdown (donors), and BM microenvironment (WT recipients). Donor mice received one injection of ENU (100 mg/kg) 2 weeks before BM harvest. Recipient mice received one injection of ENU (100 mg/kg) 3 weeks before lethal irradiation and transplantation. **B**, Percentage of GFP⁺ cells in the BM at the time of transplantation, and in the blood of mice at 1.5 and 5 months posttransplantation. There was a significantly greater percentage of GFP⁺ cells in the blood of ENU-treated mice at 1.5 month and 5 months. The *P* values from a two-tailed Student *t* test at 1.5 months are shown. At 5 months, only “donor” and “both” conditions showed a significant expansion of GFP⁺ cells ($P < 0.0001$). ENU exposure of both donor and recipient creates a more optimal environment for the expansion of *Trp53* shRNA, GFP⁺ cells. **C**, Kaplan-Meier survival curves of WT recipients transplanted with *Egr1*^{+/-}, *Apc*^{del/+} BM cells transduced with *Trp53* shRNA. When both donor and recipient mice are exposed to ENU, survival time is significantly decreased (200 days). There was no statistical difference in survival between ENU-donor versus no ENU ($P = 0.831$) or ENU-recipient versus no ENU ($P = 0.737$), or ENU-donor versus ENU recipient cohorts ($P = 0.910$). **D**, Histologic classification of diseases arising in the mice.

an increased repopulation of 95% ($P = 0.05$) suggesting that an ENU-treated microenvironment may effect *Egr1*^{+/-} stem cell fitness. Thus, alterations to the microenvironment may induce senescence of MSCs and trigger SASP, thereby creating a permissive environment that impacts stem cell fitness, and contributes to the pathogenesis of myeloid neoplasms.

Loss of *Trp53*, Concurrent with Two Del(5q) Genes, *Egr1* and *Apc*, Models High-risk MDS/AML

TP53 mutations are associated with complex karyotypes, high-risk MDS, transformation to AML, and poor overall survival (3, 4, 37). We next compared disease development in mice transplanted with *Egr1*^{+/-}, *Apc*^{del/+} BM transduced with

luciferase control shRNA cells (*EA-Luc*, black) versus *Trp53* shRNA (*EA-Trp53*, red; Fig. 4A). Both the donor and the recipient mice were treated with ENU. *EA-Luc* mice survived significantly longer (370 days vs. 200 days, $P = 0.0014$; Fig. 4A), and none developed AML (Fig. 4B). Most (93%, 13/14) developed MDS with marked proliferation of dysplastic erythroblasts, and some mild granulocytic and megakaryocytic dysplasia (Supplementary Fig. S5). In contrast, the addition of *Trp53* knockdown led to leukemia development; 45% (5/11) of *EA-Trp53* mice (red) developed AML versus none (0/14) of the *EA-Luc* mice ($P = 0.009$; Fig. 4B). Together, our data show that cell-intrinsic loss of *Egr1* and *Apc* is not sufficient to promote the development of overt leukemia, even



when HSPCs and the microenvironment are exposed to ENU. However, concordant loss of *Trp53* leads to the development of AML in almost half of the mice when both the HSPCs and microenvironment are exposed to ENU. The severity of disease appears to worsen with the additional loss of *Apc*, because *E-Trp53* mice did not succumb to disease as quickly as did *EA-Trp53* mice (369 days vs. 200 days, $P = 0.0177$; Supplementary Fig. S6A), and showed a trend towards more MDS and less AML compared with *EA-Trp53* mice (Supplementary Fig. S6B). Thus, the *EA-Trp53* mouse model mimics del(5q) MDS patients, where *TP53* mutation and/or loss confers the highest risk for disease progression and death in patients.

Several lines of evidence suggest that the *EA-Trp53* AMLs model the progression to high-risk disease. Gene expression profiling of *EA-Trp53* AML versus *EA-Luc* MDS samples revealed a positive enrichment of the hematopoiesis early progenitor signature, and a negative enrichment of the hematopoiesis mature cell and the myeloid cell maturation signatures in AML samples (Fig. 4C and D), as well as an elevated (>20%) myeloblast count, modeling the transition from MDS to AML. A strong upregulation of *MYC* target genes and WNT/ β -catenin signaling in *EA-Trp53* AML samples (Fig. 4E and F) modeled our previous expression profiling data of del(5q) t-MN patients, which showed a distinctive upregulation of the *MYC* oncogene, and deregulated WNT signaling (38, 39). In *EA-Trp53* samples, compared with *EA-Luc* MDS, there were a greater number of mice with a clonal chromosomal aberration [75% (6/8) vs. 28% (2/7), $P = 0.13$], and on average a greater number of aberrations (7 vs. 1.6, $P = 0.22$; Supplementary Table S2); however, the sample size was small and these differences did not reach statistical significance. Overall, our mouse model provides a tractable system to understand the molecular events defining del(5q) t-MNs with *TP53* deficiency (through 17p loss or *TP53* mutation) and, potentially, to test novel therapies.

Although AML samples were transplantable to secondary recipients, MDS samples (with or without *Trp53* shRNA) were not (Supplementary Table S1). The inability to transplant MDS is similar to the observation that transplantation of CD34⁺ cells from patients with MDS does not result in engraftment or propagation in murine xenograft models, unless MDS-derived MSCs, but not MSCs from age-matched healthy controls, are coinjected (16), supporting a contribution of the BM microenvironment to the pathogenesis

of MDS. In our *EA-luc* model, we noted that development of MDS was particularly sensitive to ENU's effect on the microenvironment (Fig. 5A). ENU treatment of donor *Egr1*, *Apc*^{del/+} mice exposing the HSPCs to ENU was not sufficient to promote the development of MDS (Fig. 5B). However, when WT recipient mice were treated with ENU, *EA-luc* mice developed MDS at the same penetrance and latency as when both donor and recipient were treated with ENU (80% MDS vs. 93% MDS, $P = 0.55$; 390 days vs. 374 days median MDS survival, $P = 0.271$; ENU-recipient vs. ENU-both, respectively; Fig. 5B and C). Because an expansion of erythroblasts in conjunction with morphologic dyspoiesis was observed, these data are consistent with a neoplastic rather than reactive process. These data suggests that ENU treatment of the stromal microenvironment influences disease progression of *Egr1*, *Apc*^{del/+} HSPCs resulting in MDS. Thus, chemotherapy may, in some instances, be a cell-extrinsic factor driving emergence of MDS clones.

DNA Damage Response Genes Are Somatic Mutated in AMLs Modeling Del(5q) t-MN

To identify whether loss of *Egr1*, *Apc*, and *Trp53* was sufficient to drive AML transformation, or whether additional mutations were required, we performed whole-exome sequencing (WES) on seven *EA-Luc* MDS and eight *EA-Trp53* AML samples. All seven MDS and five of eight AML samples were derived from ENU-both conditions; two AMLs were derived without ENU (1586 and 4525) and one AML (7914) after ENU treatment of the recipient only. The median number of deleterious mutations per mouse was eight (range: 0–24) for the *EA-Luc* MDS samples, and 12.5 (range: 1–40) for the *EA-Trp53* AML samples (Fig. 6A). Indel mutations were detected only in the *EA-Trp53* AML group and ranged from 0 to 3 per sample. The median variant allele frequency (VAF) was similar for the *EA-Luc* MDS and *EA*, *Trp53*-AML groups (27%, range 20–55%; and 30%, range 20–64%, respectively). A complete list of mutated genes, with a Genomic Evolutionary Rate Profiling (GERP) score >2 and considered to be deleterious, is found in Supplementary Table S3.

Mutated genes were categorized into the 10 functional categories of genes that are recurrently mutated in MDS and AML: genes encoding chromatin modifiers, DNA methylation regulators, DNA repair proteins, ribosomal proteins, signal transducers, transcription factors, tumor suppressors,

Figure 3. ENU induces senescence of mesenchymal stromal cells. **A** and **B**, MSCs were treated with varying doses of ENU for 24 hours *in vitro*. Seven days later, cells were either stained for SA- β -gal or incubated 24 hours with EdU, then fixed and stained. Five and three independent experiments were done for SA- β -gal and EdU, respectively. A senescence-inducing dose of 10 Gy was used as a positive control. **C**, Quantitative PCR analysis of RNA isolated from control (10% ethanol) and ENU-treated (0.2 mg/mL) MSCs at day 7. Values are presented as a ratio of target mRNA to 18S rRNA. $N = 3$ independent experiments, each done in triplicate. **D–H**, Mice were mock-treated (10% ethanol) or ENU-treated (100 mg/kg). One month later, mice were sacrificed and MSCs were isolated. **D** and **E**, The CFU-F assay was used to estimate the proliferative and clonogenic potential of MSCs. MSCs were isolated from collagenase-treated compact bones and either directly plated (**D**) or passaged once (**E**) before plating. $N = 5$ and 9 independent experiments for **D** and **E**, respectively. **F–H**, Early passage MSCs (P1–2) were stained for SA- β -gal or harvested for RNA. $N = 3$ independent experiments. Significant differences between control (no ENU/mock) and experimental were calculated by two-tailed Student t test for **A–F**. *, $P < 0.05$; **, $P < 0.001$; ***, $P < 0.0001$. **G** and **H**, GSEA of MSCs from ENU-treated versus mock-treated mice shows an enrichment of the p53 pathway and specific SASP factors, shown below enrichment plot. **I**, Equal numbers of *Egr1*^{+/+}(WT) or *Egr1*^{+/-}(CD45.2) and WT B6.SJL competitor cells (CD45.1) were transplanted into lethally irradiated recipients that were mock- or ENU-treated, 3 weeks before transplantation. Ratios of CD45.2 (*Egr1*^{+/+} or *Egr1*^{+/-}) versus competitor (CD45.1) for short-term hematopoietic stem cells (ST-HSC; Lin⁻ Sca1⁺ Kit⁺ CD48⁻ CD150⁻) were calculated 4 months posttransplant. A repopulation ratio of CD45.2 (WT-*Egr1*^{+/+}) to CD45.1 in mock-treated conditions was set to 1 (expressed as 100%). Without ENU, *Egr1*^{+/-} ST-HSC showed an average repopulation frequency of 31%; with ENU treatment, repopulation increased to 95% ($P = 0.05$ by two-tailed Student t test) suggesting that an ENU-treated microenvironment impacts stem cell fitness.

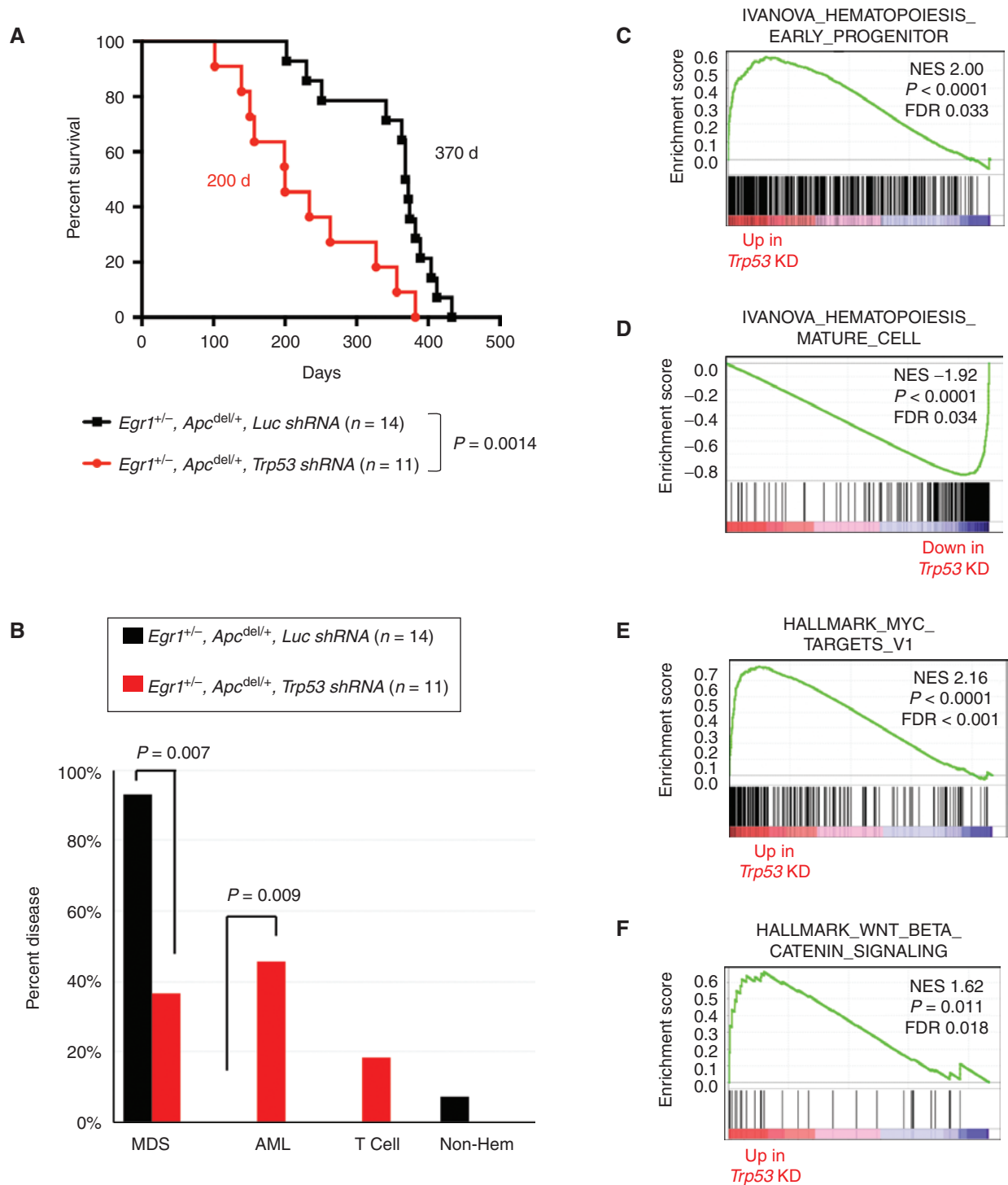


Figure 4. Following exposure to an alkylating agent, haploinsufficiency of both *Egr1* and *Apc* promotes development of MDS; loss of these genes together with *Trp53* promotes AML development. **A**, Kaplan-Meier survival curves of WT recipients transplanted with *Egr1*^{+/-}, *Apc*^{del/+} BM cells transduced with *Luc* shRNA (EA-*Luc*: black) or *Trp53* shRNA (EA-*Trp53*: red). Both donor and recipient mice were treated with ENU. Disease development is significantly faster in EA-*Trp53* mice compared with EA-*Luc* mice (200 days vs. 370 days, $P = 0.0014$). **B**, Histologic classification of diseases shows that most EA-*Luc* mice developed MDS, and none developed AML. **C-F**, Mouse genes were collapsed to human gene names; differentially expressed genes in EA-*Trp53* AML samples (n = 6) versus EA-*Luc* MDS samples (n = 6) were analyzed using the GSEA software. Features, such as a block in myeloid differentiation and upregulation of MYC target genes and WNT/ β -catenin signaling recapitulate human t-MN.

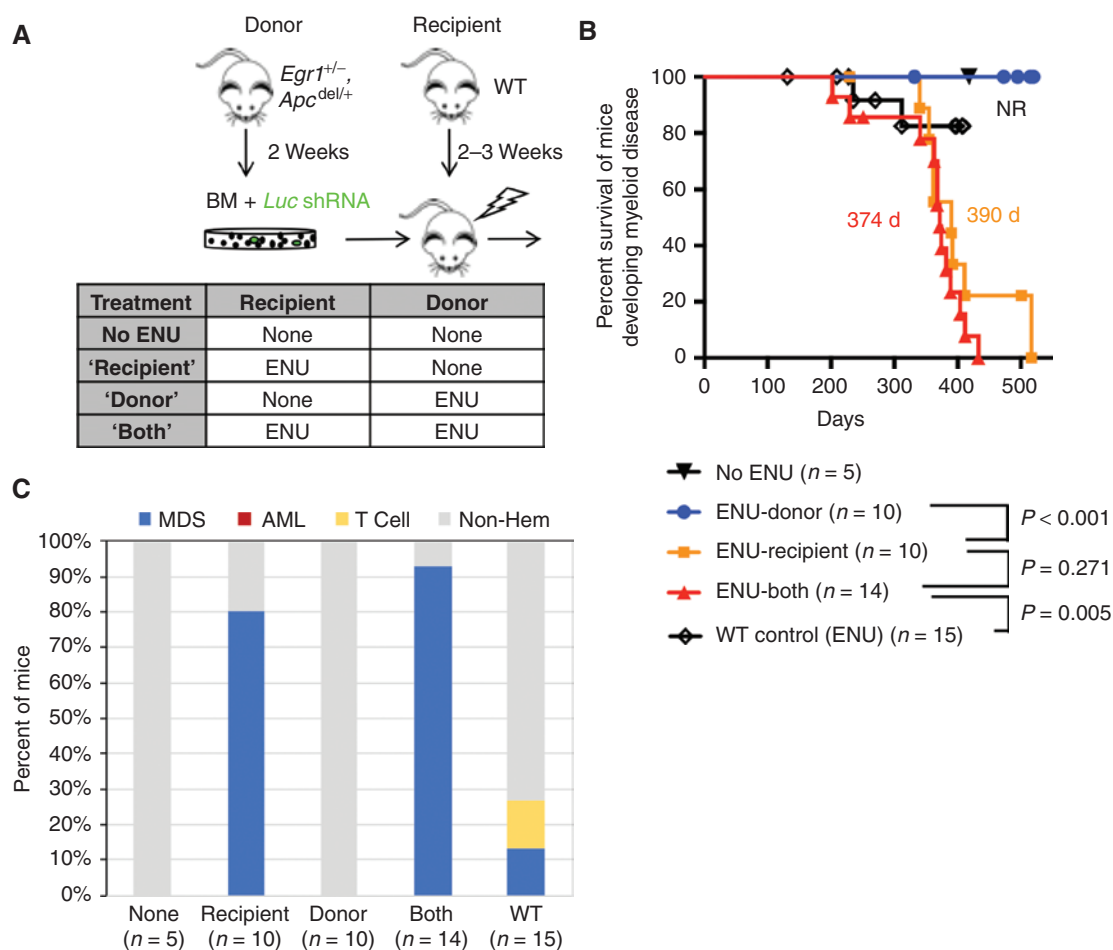


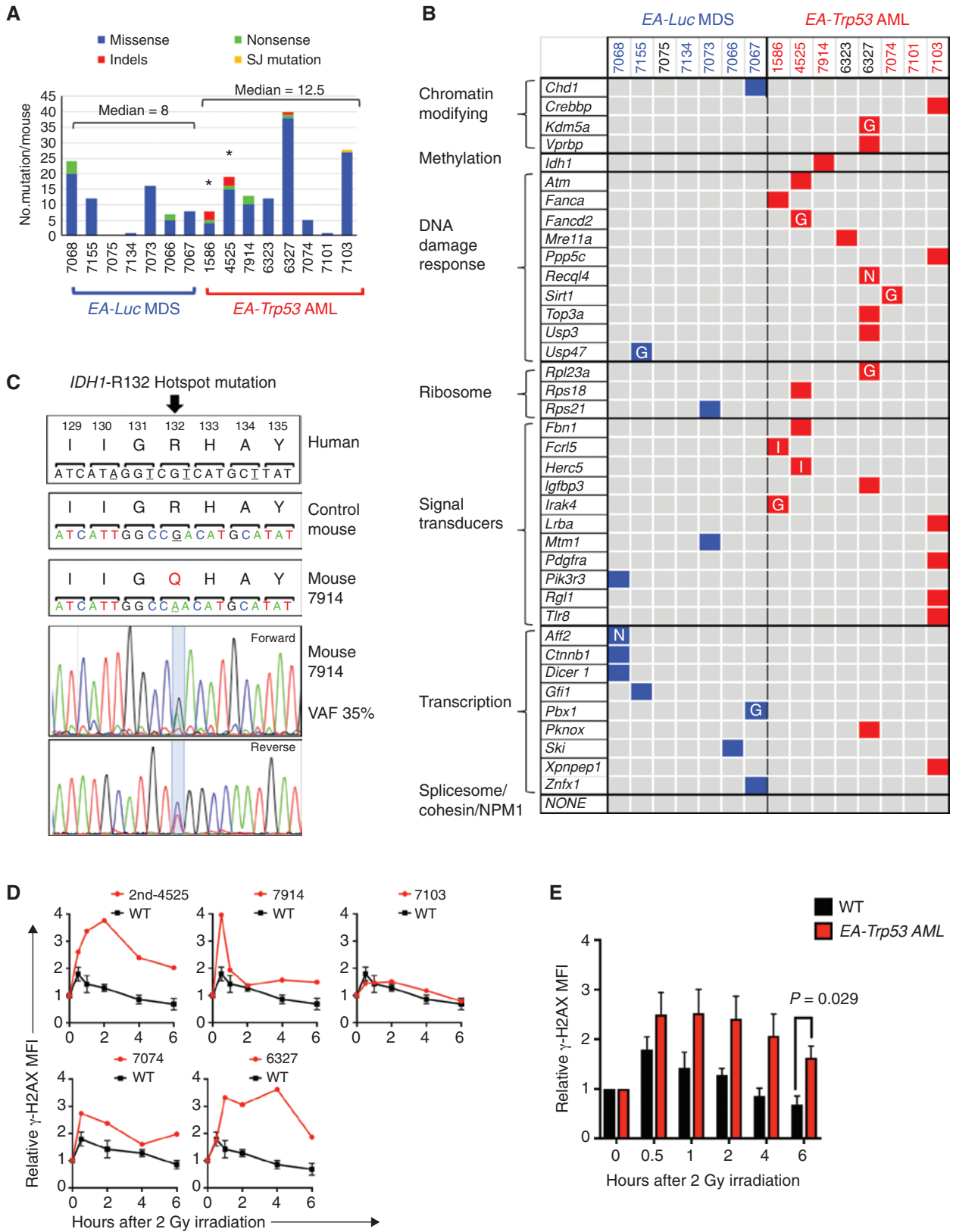
Figure 5. ENU exposure of the BM microenvironment is a major force driving MDS development in mice transplanted with *Egr1* and *Apc* haploinsufficient HSPCs. **A**, Schematic of the transplantation schemes used to elucidate the effects of alkylating agents on HSPCs (donor) versus the microenvironment (recipient) in the absence of *Trp53* knockdown. WT recipients were transplanted with *Egr1*^{+/-}, *Apc*^{del/+} BM cells transduced with *Luc* shRNA (control) under 4 different ENU conditions. Donor mice received one injection of ENU (100 mg/kg) 2 weeks before bone marrow harvest. Recipient mice received one injection of ENU (100 mg/kg) 3 weeks before lethal irradiation and transplantation. **B**, Kaplan-Meier survival curves of mice developing myeloid disease. Survival time is similar when only recipient mice are exposed (390 days) versus when both donor and recipient mice are exposed to ENU (374 days; $P = 0.271$). As a control, WT BM was transplanted into WT recipients, and then treated with ENU; median survival was not reached as only 2 of 15 (13%) mice developed MDS. **C**, Histologic classification of diseases arising in the mice. The percent of mice that developed MDS in ENU-recipient (80%) and ENU-both (93%) conditions was similar ($P = 0.55$ by Fisher exact test).

cohesin and spliceosome components, and *NPM1* (refs. 40, 41; Fig. 6B). There were two nonsense mutations (*Recql4*, *Aff2*) and two indel mutations (*Fcrl5*, *Herc5*); the remaining missense mutations were considered to be deleterious by the GERP, Sorting Tolerant from Intolerant (SIFT) and/or Polymorphism Phenotyping v2 (PolyPhen-2) algorithms (Fig. 6B; Supplementary Table S4). Interestingly, six similar missense gene mutations (*Idh1*, *Atm*, *Lrba*, *Pdgfra*, *Pik3r3*, and *Dicer*) were identified in human patients using the Clinvar database.

Within the ten categories listed above, there was a significantly greater number of genes mutated in the *EA*, *Trp53*-AML versus *EA-Luc* MDS group (26 vs. 12, $P = 0.0026$ by Fisher exact test). Ribosomal and signaling genes were mutated in both groups, with signaling gene mutations occurring more frequently in *EA-Trp53* AML samples ($P = 0.0089$). Genes encoding transcription factors were mutated more frequently in *EA-Luc* MDS samples ($P = 0.057$). The chromatin modify-

ing (*Crebbp*, *Kdm5a*, and *Vprbp*) and DNA methylation (*Idh1*) genes were mutated in *EA*, *Trp53*-AMLs. Mutations in genes encoding cohesin or spliceosome components or *Npm1*, which are not enriched in the del(5q) subgroup of t-MN (1), were not detected.

Investigation of the mutated genes with the Molecular Signatures Database revealed that there was a significant enrichment of genes within the Gene Ontology (GO)_DNA repair ($P = 1.18 \times 10^{-8}$) collection and include *Atm*, *Fanca*, *Fancd2*, *Mre11a*, *Ppp5c*, *Recql4*, *Sirt1*, *Top3a*, *Usp3*, and *Usp47* (Supplementary Table S5). Remarkably, a significantly larger number of DNA damage response (DDR) gene mutations were in the *EA-Trp53* AML versus the *EA-Luc* MDS group ($P = 0.0003$, Fisher exact test). In addition, *Idh1* mutations have been linked to altered DNA repair (42), and mouse 7914 had a somatic *Idh1* mutation that corresponded with the *IDH1* mutation involving arginine 132 (R132 “hotspot”)



frequently observed in human malignancies (Fig. 6C). Mutations were confirmed by Sanger sequencing (Supplementary Fig. 7). Figure 6B illustrates that each *EA-Trp53* AML had at least one mutation in a DNA repair gene (with the exception of mouse 7101). Somatic mutations in *IDH1* and *ATM*, and germline mutations in Fanconi anemia genes have been observed in patients with t-MN (refs. 29, 43; Supplementary Table S6). In AML samples from patients, curated by the Catalogue Of Somatic Mutations In Cancer (COSMIC) database, there are codon-altering mutations in *IDH1*, *ATM*, *FANCA*, *MRE11*, *RECQL5*, *USP3*, and *USP47*; *FANCD2*, *PPP5C*, *TOP3A* are mutated only in lymphoid neoplasms (Supplementary Table S6). These findings support the hypothesis that mutation of the DDR genes identified in *EA-Trp53* AMLs contributes to the development of myeloid disease.

To test for a defect in the DNA damage response, we measured the induction and resolution of phosphorylated histone H2AX (γ H2AX), a well-established marker for DSBs, after 2 Gy of irradiation, and showed that cells from 4 of 5 *EA-Trp53* AMLs tested have an aberrant double-strand break response (as measured by resolution of γ H2AX fluorescence), similar to our previously published results (ref. 6; Fig. 6D). Cells from one leukemia mouse (7103) had a normal γ H2AX response even though they had a mutation in the *Ppp5c* gene, which encodes a serine/threonine phosphatase involved in multiple cellular processes, including the DNA damage response. At 6 hours postirradiation, the mean fluorescence intensity of γ H2AX was approximately 2.4-fold higher in *EA-Trp53* AML samples suggesting that AML cells are unable to resolve DSBs to the same extent as WT cells (Fig. 6E). Thus, haploinsufficiency of two critical del(5q) genes, *Egr1* and *Apc*, with concurrent *Trp53* loss is sufficient to initiate disease; however, acquisition of a DDR gene mutation, and ensuing abnormal DNA repair response, appears to be critical for transformation to AML.

DISCUSSION

In this study, we addressed the long-standing question of the role of cytotoxic therapy in the pathogenesis of t-MN, and why prior cytotoxic therapy strongly selects for *TP53* loss and/or mutation in conjunction with a del(5q). We

showed that loss of *Trp53* in HSPCs in conjunction with two key tumor suppressor del(5q) genes, *Egr1* and *Apc*, was required for the development of AML; the development of AML was associated with the acquisition of deleterious mutations in DNA repair genes. Modeling the consequence of a cytotoxic-exposed microenvironment, our data suggest that chemotherapy-induced alterations to the microenvironment should be considered one of the predisposing risk factors for the development of t-MN. Although the seminal study by Wong and colleagues demonstrated that selection of cells with *TP53* mutations/loss occurs after exposure to DNA-damaging chemotherapeutics (11), this study did not distinguish the effect of chemotherapy on HSPCs versus the microenvironment. Our *in vivo* model shows the unexpected finding that a chemotherapy-exposed microenvironment promotes this expansion. Moreover, we introduce the concept that senescent phenotype within the BM microenvironment, induced by prior cytotoxic therapy, may contribute to the pathogenesis of t-MN.

Jacoby and colleagues previously demonstrated that myeloblasts from the majority of patients with t-MN are characterized by deregulation of the DNA damage response, even though few somatically mutated DDR genes were identified (14). It is striking that in our model of del(5q) t-MN, leukemia development in mice selected for mutations of DDR genes, impairing the DDR, similar to patients with t-MN. The results of our studies suggest that *TP53* loss, on its own, does not lead to an impaired DNA damage response in t-MN, because nearly every mouse AML with *Trp53* loss had acquired a mutation of a DDR gene. Although patients with t-MN do not generally exhibit somatically mutated DDR genes (1), inherited and acquired mutations, epigenetic modifications, and/or chromosomal loss of DNA repair gene(s) may all contribute to an aberrant DNA damage response in patients. The finding that the AML developing in mice selected for DDR gene mutations in a model of t-MN lends support to the idea that therapeutic approaches exploiting a dysfunctional double-strand break response should be considered for t-MN.

A new paradigm in leukemogenesis is that alterations of the microenvironment contribute to the pathogenesis of myeloid malignancies (15, 17, 18, 44). This may be due to genetic

Figure 6. Enrichment of DNA repair gene mutations in myeloid neoplasms with *Trp53* knockdown. **A**, Summary of nonsynonymous mutations in 7 *EA-Luc* MDS and 8 *EA, Trp53*-AML samples. Both donor and recipient mice were treated with ENU with the exception of 3 mice: 1586 and 4525 (no ENU); 7914 (ENU recipient alone). All *EA, Trp53* mice had a >20% blast count, except 6327, which had 18% blasts. The median number of mutations was not statistically different in the *EA-Luc* MDS versus the *EA-Trp53* AML group (8 vs. 12.5). Two *EA, Trp53*-AMLs (1586, 4525), which arose without ENU treatment (*) had a median of 13.5 mutations. **B**, Because there were no genes that were mutated in multiple mice, mutations were classified into 10 gene categories that are commonly mutated (somatic and inherited) in patients with MDS or AML. Colored boxes identify genes that are mutated in each mouse. Nonsense (N) and indel (I) mutations are indicated. Most missense mutations were considered to be pathogenic by at least two of the following algorithms: GERP, SIFT, and PolyPhen2 (Supplementary Table S4). Missense mutations considered pathogenic by GERP score alone are indicated by the letter "G." With the exception of 7101, all *EA, Trp53*-AMLs harbor a mutation in a gene within the gene ontology term "DNA repair." Bone marrow samples from mice identified in blue and red numbering were used for RNA-seq analysis. **C**, The normal nucleotide and amino acid sequence and position (human) of the *IDH1* gene are shown in the upper panels. The amino acid sequence is conserved in this region. Mouse 7914 had a mutation at the R132 position, which is a hotspot mutation in humans. The chromatograms with the mutation are shown. **D**, γ H2AX levels were measured in CD117 (Kit)⁺ (4525-2nd, 7914) or CD11b⁺ (7074, 6327, 7103, 7098) cells at baseline, and up to 6 hours post 2 Gy irradiation (4525-2nd and 7914 expressed Kit, but not CD11b). We previously showed that leukemia cells from 1586 and 4525 have an aberrant DNA damage response (6). AML that arose in a secondary transplant using 4525 donor cells (4525-2nd sample) also showed a defective DNA repair response. The mean fluorescence intensity measured using flow cytometry, was normalized to the 0-hour time point for each sample, to compare the induction and resolution kinetics among samples. Kinetics of each AML sample is shown in comparison to the average kinetics of CD11b⁺ wild-type cells. We could not assess the DNA damage response in 7101 (no DDR mutation), because the irradiation did not induce a γ H2AX signal at any time point. **E**, The mean γ H2AX levels for WT ($n = 3$) and *EA, Trp53*-AML ($n = 5$) samples \pm SEM are shown. An independent, two-tailed t test was performed for each time point. The difference was statistically significant at the 6-hour time point.

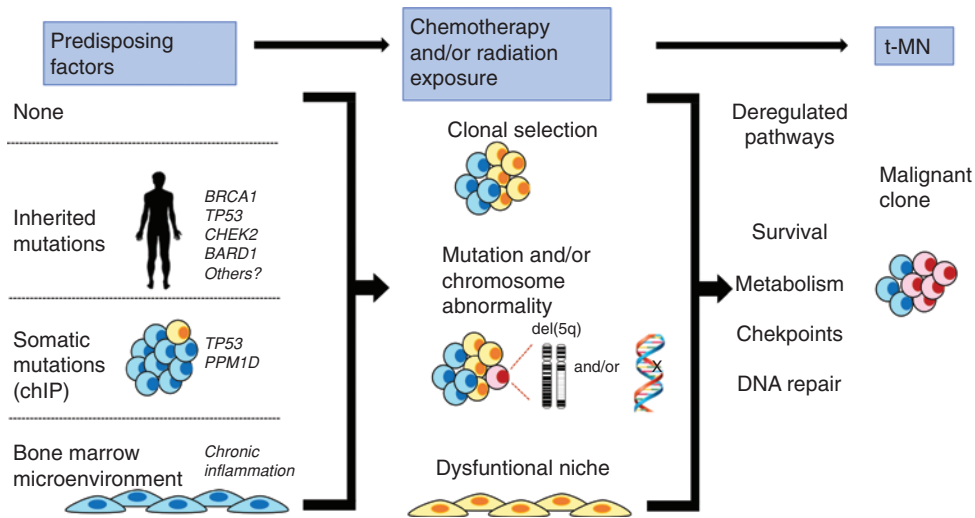


Figure 7. Model illustrating how multiple, converging pathways may lead to t-MN. Left, various predisposing factors that may influence whether a patient develops t-MN. A patient may have no predisposing factors, have an inherited mutation (predisposing them to aberrant DNA repair), have a preexisting somatic mutation (CHIP), or have an aberrant BM microenvironment (due to aging and/or chronic inflammation). Middle, how multiple cycles of cytotoxic therapy may promote clonal expansion of cells with preexisting and/or newly acquired mutations and alter the BM microenvironment, possibly via therapy-induced senescence. Together, this creates permissive conditions for malignant transformation of hematopoietic cells. Right, how these changes converge to deregulate the DNA damage response and cell-cycle checkpoint, as well as enhance metabolism and survival, ultimately leading to t-MN.

alterations, as is the case for the Shwachman–Bodian–Diamond syndrome gene, remodeling of the niche by malignant myeloid cells (16, 25), or environmental exposures such as cytotoxic therapy, as suggested by this study. We hypothesize that MSCs in the BM microenvironment are key players, because recipient mice were lethally irradiated, leading to cell death of immune cells but not the MSCs, which are typically radioresistant. Although chemotherapy is known to transiently increase proinflammatory cytokines (45), we waited two weeks after ENU administration before transplanting mice. Because ENU treatment of recipient mice appeared to “set the stage” for malignant transformation, only observed months later, we hypothesized that chemotherapy must have long-term consequences on BM stromal cells, such as establishing a senescent phenotype. In support of this, senescence of nontumor cells, following doxorubicin treatment, was shown to play a key role in cancer relapse and spread to other tissues in a mouse model of breast cancer (33). Our study expands on this idea and suggests that cytotoxic therapy for a prior malignancy may have long-term effects on the microenvironment, possibly through the induction of senescence, creating an inflammatory environment and favorable conditions for the development of t-MN. Consistent with our hypothesis, it was recently shown that MSCs from t-MN patients had a higher senescent rate as compared with MSCs isolated from healthy controls, patients with primary MDS, and patients with two unrelated cancers, without prior cytotoxic exposure (46).

In Fig. 7, we propose that there are several pathways that lead to t-MN. Various predisposing factors may influence whether a patient develops t-MN (left; ref. 1). The presence of a germline mutation in genes involved in DNA repair and/or DNA damage-sensing pathways, such as *BRCA1*, *BRCA2*, *CHEK2*, *TP53*, and Fanconi anemia genes, has been identified in some patients with t-MN, and may lead to ineffective

DNA repair following cytotoxic therapy and the acquisition of somatic mutations (43, 47–49). Individuals who have CHIP, or small preexisting, age-related resilient clones, may be at increased risk of developing t-MN following cytotoxic therapy (9–13). Finally, it is also possible that the bone marrow microenvironment is damaged prior to cytotoxic therapy, due to aging, infection, chronic inflammation, or inherited mutations (50). No recurrent somatic mutations or karyotypic abnormalities have been found in MDS-derived MSCs (51). Rather, it has been proposed that malignant stromal alterations may be of an epigenetic nature (52); however, at present, it is not known if alterations precede disease or are induced by malignancy, and how chemotherapy may impact these epigenetic changes.

Our model suggests that multiple cycles of cytotoxic therapy may create conditions that promote clonal expansion of cells with preexisting and/or newly acquired mutations and/or chromosomal aberrations. Cytotoxic therapy may also alter the BM microenvironment, possibly through therapy-induced senescence, to help promote malignant transformation in t-MN. Consistent with this idea, senescence-associated changes have been observed in MSCs isolated from patients with MDS and AML (20, 25). The pathways illustrated in Fig. 7 are not mutually exclusive, and one or multiple pathways may ultimately lead to decreased DDR, deficient checkpoint responses, and alterations to metabolism, collectively contributing to increased survival and expansion of the t-MN clone. Our results suggest that niche-based therapeutic approaches, most likely in conjunction with approaches targeting the hematopoietic cells, should be considered. Thus, elucidating the effects of cytotoxic therapy on the BM microenvironment and on the HSPCs, as well as the contribution of an aberrant DNA damage response, may provide insights relevant to the development of targeted therapies for t-MN.

METHODS

Mice

All mouse studies were approved by The University of Chicago's Institutional Animal Care and Use Committee (IACUC), and mice were housed in a facility fully accredited by the Association for Assessment and Accreditation of Laboratory Animal Care. *Egr1^{+/-}*, *Mx1-Cre⁺Apc^{fl/+}* (*Egr1^{+/-}*) and *Egr1^{+/-}*, *Mx1-Cre⁺Apc^{fl/+}* (*Egr1^{+/-}*, *Apc^{del/+}*), mice were generated by crossing *Mx1-Cre* transgenic mice with *Egr1^{+/-}*, *Apc^{fl/fl}* mice (C57Bl/6 genetic background) as described previously (6).

Mouse Model of MDS/AML

Total BM cells, isolated from 10- to 12-week old *Egr1^{+/-}* or *Egr1^{-/-}*, *Apc^{del/+}* mice, were transduced with a *Luc* (control) or *Trp53*-specific shRNA (p53.1224; ref. 6) and transplanted, via retro-orbital injection, into lethally irradiated (8.6 Gy) WT mice (B6.SJL/Cd45.1). Where indicated, donor mice were injected once with ENU (100 mg/kg) 2 weeks after polyinosinic:polycytidylic acid (pI-pC) injections to induce the deletion of the floxed *Apc* allele, and recipient mice were injected once with ENU (100 mg/kg) two weeks before transplantation. In ENU, "both" conditions, *Mx1-Cre⁺Apc^{fl/+}* mice were used as WT recipient mice, instead of B6.SJL/Cd45.1 mice. Peripheral blood, histology, spectral karyotyping, and flow cytometric analyses were performed as described previously (6). To ensure that we were not biasing the disease phenotype, animals were euthanized when they displayed at least four of the following symptoms: poor grooming, abnormal hunched posture, decreased activity, listlessness or lethargy, a body conditioning score of 2 (lean), anemia (Hb < 8 g/dL), leukocytosis (> 25 K/ μ L), or thrombocytopenia (< 500 K/ μ L), and enlarged spleen, thymus, or masses (by palpation). Survival times (time to sacrifice) were estimated by the Kaplan-Meier method and compared between groups via log-rank test.

WES and RNA-seq

Exome libraries were generated using the SureSelectXT Mouse All Exon kit (Agilent, Santa Clara, CA) following the manufacturer's directions. 100 bp paired-end sequencing was performed on a HiSeq 4000 sequencing system. Reads were assessed for quality (Short Read and FastQC), overlapping reads were merged using FLASH (ver 1.2.11) and aligned to mm9 using BWA (ver 0.7.12; ref. 53). SAMtools v0.1.18 (53) was used to remove duplicates, and GATK was used for local realignment and score recalibration (54). Mutation calling was performed with reads with mapping qualities ≥ 30 , requiring $\geq 8\times$ coverage in both tumor and normal DNA (*Egr1^{+/-}*, *Apc^{fl/+}*) requiring a variant read on each strand, and a minimum VAF of 20%. Indels identified using VarScan v2.3.4 (55), and single nucleotide mutations identified using both MuTect v1.1.4 (56) and VarScan were retained. Known single-nucleotide polymorphisms (SNP) for the C57Bl/6 strain were removed. Only mutations with a GERP score (57) >2 predicted to have deleterious consequences were included. All gene mutations listed in Fig. 5B were validated by Sanger sequencing. RNA-seq analysis was performed as described, with the exception that reads were aligned to mm10 and the MSC dataset was pseudoaligned with Kallisto (58). Sequencing data are available on the Gene Expression Omnibus database (GSE135866) and Sequence Read Archive (PRJNA597332).

MSC Senescence Assays

To isolate MSCs, femur, tibia, and humerus bones were flushed to remove hematopoietic cells, treated with collagenase, and cultured using MesenCult (Mouse) with MesenPure in 5% O₂ according to the manufacturer's recommendations (Stemcell Technologies). To measure SA- β -gal that is detectable at pH 6 (due to increased lysosomal biogenesis in senescent cells), the internal pH of lysosomes was increased to approximately pH 6 using bafilomycin A1. Cells

were then incubated with 5-dodecanoylaminofluorescein di- β -D-galactopyranoside (C₁₂FDG; Cayman Chemicals), a β -galactosidase substrate that becomes fluorescent after cleavage by the enzyme. SA- β -gal activity was estimated using flow cytometry. Cell proliferation was assayed with the EZClick EdU proliferation kit (BioVision, Inc.). For colony-forming units-fibroblastic (CFU-F) assays, either 2×10^4 directly isolated MSCs (postcollagenase) or 2×10^3 first-passage MSCs were plated per well of a 6-well plate, and stained with 0.5% crystal violet after 14 days to enumerate colonies. Quantitative PCR was performed as described previously (59). Primer sequences are provided in Supplementary Table S7. For RNA-seq analysis, MSCs were isolated from mock- or ENU-treated mice, approximately 1 month posttreatment, and expanded *in vitro* to passage 1 or 2.

Disclosure of Potential Conflicts of Interest

M.M. Le Beau is a member, board of directors at Varian Medical Systems and is a consultant/advisory board member for American Cancer Society and Leukemia and Lymphoma Society. No potential conflicts of interest were disclosed by the other authors.

Authors' Contributions

A. Stoddart: Conceptualization, data curation, formal analysis, supervision, investigation, methodology, writing—original draft, project administration, writing—review, and editing. **J. Wang:** Investigation. **A.A. Fernald:** Investigation. **E.M. Davis:** Investigation. **C.R. Johnson:** Investigation. **C. Hu:** Investigation. **J.X. Cheng:** Formal analysis. **M.E. McNERNEY:** Supervision, writing—review, and editing. **M.M. Le Beau:** Conceptualization, supervision, funding acquisition, writing—original draft, writing—review, and editing.

Acknowledgments

This work was supported by a Public Health Service, National Institutes of Health, National Cancer Institute grant (RO1 CA190372), and a grant from the Edward P. Evans Foundation (to M.M. Le Beau), as well as the Genomics Core Facility and the Cytometry and Antibody Technology Facility of The University of Chicago Medicine Comprehensive Cancer Center (P30 CA014599). M.E. McNERNEY is supported by RO1 CA231880, the American Cancer Society Research Scholar Award, and The Brinson Foundation.

We would like to thank the Le Beau and McNERNEY laboratory members for the insightful discussions about this research project, and the University of Chicago Biostatistics Core Facility for providing statistical support.

The costs of publication of this article were defrayed in part by the payment of page charges. This article must therefore be hereby marked *advertisement* in accordance with 18 U.S.C. Section 1734 solely to indicate this fact.

Received August 13, 2019; revised December 19, 2019; accepted March 12, 2020; published first April 20, 2020.

REFERENCES

- McNERNEY ME, Godley LA, Le Beau MM. Therapy-related myeloid neoplasms: when genetics and environment collide. *Nat Rev Cancer* 2017;17:513–27.
- Smith SM, Le Beau MM, Huo D, Karrison T, Sobeks RM, Anastasi J, et al. Clinical-cytogenetic associations in 306 patients with therapy-related myelodysplasia and myeloid leukemia: the University of Chicago series. *Blood* 2003;102:43–52.
- Christiansen DH, Andersen MK, Pedersen-Bjergaard J. Mutations with loss of heterozygosity of p53 are common in therapy-related myelodysplasia and acute myeloid leukemia after exposure to

- alkylating agents and significantly associated with deletion or loss of 5q, a complex karyotype, and a poor prognosis. *J Clin Oncol* 2001;19:1405–13.
4. Lindsley RC, Mar BG, Mazzola E, Grauman PV, Shareef S, Allen SL, et al. Acute myeloid leukemia ontogeny is defined by distinct somatic mutations. *Blood* 2015;125:1367–76.
 5. Jerez A, Gondek LP, Jankowska AM, Makishima H, Przychodzen B, Tiu RV, et al. Topography, clinical, and genomic correlates of 5q myeloid malignancies revisited. *J Clin Oncol* 2012;30:1343–9.
 6. Stoddart A, Fernald AA, Wang J, Davis EM, Karrison T, Anastasi J, et al. Haploinsufficiency of del(5q) genes, Egr1 and Apc, cooperate with Tp53 loss to induce acute myeloid leukemia in mice. *Blood* 2014;123:1069–78.
 7. Jaiswal S, Fontanillas P, Flannick J, Manning A, Grauman PV, Mar BG, et al. Age-related clonal hematopoiesis associated with adverse outcomes. *N Engl J Med* 2014;371:2488–98.
 8. Xie M, Lu C, Wang J, McLellan MD, Johnson KJ, Wendl MC, et al. Age-related mutations associated with clonal hematopoietic expansion and malignancies. *Nat Med* 2014;20:1472–8.
 9. Gillis NK, Ball M, Zhang Q, Ma Z, Zhao Y, Yoder SJ, et al. Clonal haemopoiesis and therapy-related myeloid malignancies in elderly patients: a proof-of-concept, case-control study. *Lancet Oncol* 2017;18:112–21.
 10. Takahashi K, Wang F, Kantarjian H, Doss D, Khanna K, Thompson E, et al. Preleukaemic clonal haemopoiesis and risk of therapy-related myeloid neoplasms: a case-control study. *Lancet Oncol* 2017;18:100–11.
 11. Wong TN, Ramsingh G, Young AL, Miller CA, Touma W, Welch JS, et al. Role of TP53 mutations in the origin and evolution of therapy-related acute myeloid leukaemia. *Nature* 2015;518:552–5.
 12. Wong TN, Miller CA, Jotte MRM, Bagegni N, Baty JD, Schmidt AP, et al. Cellular stressors contribute to the expansion of hematopoietic clones of varying leukemic potential. *Nat Commun* 2018;9:455.
 13. Lindsley RC, Saber W, Mar BG, Redd R, Wang T, Haegenson MD, et al. Prognostic mutations in myelodysplastic syndrome after stem-cell transplantation. *N Engl J Med* 2017;376:536–47.
 14. Jacoby MA, De Jesus Pizarro RE, Shao J, Koboldt DC, Fulton RS, Zhou G, et al. The DNA double-strand break response is abnormal in myeloblasts from patients with therapy-related acute myeloid leukemia. *Leukemia* 2014;28:1242–51.
 15. Kode A, Manavalan JS, Mosialou I, Bhagat G, Rathinam CV, Luo N, et al. Leukaemogenesis induced by an activating beta-catenin mutation in osteoblasts. *Nature* 2014;506:240–4.
 16. Medyouf H, Mossner M, Jann JC, Nolte F, Raffel S, Herrmann C, et al. Myelodysplastic cells in patients reprogram mesenchymal stromal cells to establish a transplantable stem cell niche disease unit. *Cell Stem Cell* 2014;14:824–37.
 17. Raaijmakers MH, Mukherjee S, Guo S, Zhang S, Kobayashi T, Schoonmaker JA, et al. Bone progenitor dysfunction induces myelodysplasia and secondary leukaemia. *Nature* 2010;464:852–7.
 18. Stoddart A, Wang J, Hu C, Fernald AA, Davis EM, Cheng JX, et al. Inhibition of WNT signaling in the bone marrow niche prevents the development of MDS in the Apcdel/+ MDS mouse model. *Blood* 2017;129:2959–70.
 19. Zambetti NA, Ping Z, Chen S, Kenswil KJ, Mylona MA, Sanders MA, et al. Mesenchymal inflammation drives genotoxic stress in hematopoietic stem cells and predicts disease evolution in human pre-leukemia. *Cell Stem Cell* 2016;19:613–27.
 20. Mattiucci D, Maurizi G, Leoni P, Poloni A. Aging- and senescence-associated changes of mesenchymal stromal cells in myelodysplastic syndromes. *Cell Transplant* 2018;27:754–64.
 21. Fei C, Zhao Y, Guo J, Gu S, Li X, Chang C. Senescence of bone marrow mesenchymal stromal cells is accompanied by activation of p53/p21 pathway in myelodysplastic syndromes. *Eur J Haematol* 2014;93:476–86.
 22. Kornblau SM, Ruvolo PP, Wang RY, Battula VL, Shpall EJ, Ruvolo VR, et al. Distinct protein signatures of acute myeloid leukemia bone marrow-derived stromal cells are prognostic for patient survival. *Haematologica* 2018;103:810–21.
 23. Geyh S, Oz S, Cadeddu RP, Frobel J, Bruckner B, Kundgen A, et al. Insufficient stromal support in MDS results from molecular and functional deficits of mesenchymal stromal cells. *Leukemia* 2013;27:1841–51.
 24. Zhao Y, Wu D, Fei C, Guo J, Gu S, Zhu Y, et al. Down-regulation of Dicer1 promotes cellular senescence and decreases the differentiation and stem cell-supporting capacities of mesenchymal stromal cells in patients with myelodysplastic syndrome. *Haematologica* 2015;100:194–204.
 25. Abdul-Aziz AM, Sun Y, Hellmich C, Marlein CR, Mistry J, Forde E, et al. Acute myeloid leukemia induces protumoral p16INK4a-driven senescence in the bone marrow microenvironment. *Blood* 2019;133:446–56.
 26. Calkoen FG, Vervat C, van Pel M, de Haas V, Vijfhuizen LS, Eising E, et al. Despite differential gene expression profiles pediatric MDS derived mesenchymal stromal cells display functionality in vitro. *Stem Cell Res* 2015;14:198–210.
 27. Joslin JM, Fernald AA, Tennant TR, Davis EM, Kogan SC, Anastasi J, et al. Haploinsufficiency of EGR1, a candidate gene in the del(5q), leads to the development of myeloid disorders. *Blood* 2007;110:719–26.
 28. Wang J, Fernald AA, Anastasi J, Le Beau MM, Qian Z. Haploinsufficiency of Apc leads to ineffective hematopoiesis. *Blood* 2010;115:3481–8.
 29. Shih AH, Chung SS, Dolezal EK, Zhang SJ, Abdel-Wahab OI, Park CY, et al. Mutational analysis of therapy-related myelodysplastic syndromes and acute myelogenous leukemia. *Haematologica* 2013;98:908–12.
 30. Kogan SC, Ward JM, Anver MR, Berman JJ, Brayton C, Cardiff RD, et al. Bethesda proposals for classification of nonlymphoid hematopoietic neoplasms in mice. *Blood* 2002;100:238–45.
 31. Subramanian A, Tamayo P, Mootha VK, Mukherjee S, Ebert BL, Gillette MA, et al. Gene set enrichment analysis: a knowledge-based approach for interpreting genome-wide expression profiles. *Proc Natl Acad Sci U S A* 2005;102:15545–50.
 32. Li L, Li M, Sun C, Francisco L, Chakraborty S, Sabado M, et al. Altered hematopoietic cell gene expression precedes development of therapy-related myelodysplasia/acute myeloid leukemia and identifies patients at risk. *Cancer Cell* 2011;20:591–605.
 33. Demaria M, O'Leary MN, Chang J, Shao L, Liu S, Alimirah F, et al. Cellular senescence promotes adverse effects of chemotherapy and cancer relapse. *Cancer Discov* 2017;7:165–76.
 34. Campisi J, d'Adda di Fagnaga F. Cellular senescence: when bad things happen to good cells. *Nat Rev Mol Cell Biol* 2007;8:729–40.
 35. Coppe JP, Desprez PY, Krtolica A, Campisi J. The senescence-associated secretory phenotype: the dark side of tumor suppression. *Annu Rev Pathol* 2010;5:99–118.
 36. Min IM, Pietramaggiore G, Kim FS, Passegue E, Stevenson KE, Wagers AJ. The transcription factor EGR1 controls both the proliferation and localization of hematopoietic stem cells. *Cell Stem Cell* 2008;2:380–91.
 37. Ok CY, Patel KP, Garcia-Manero G, Routbort MJ, Fu B, Tang G, et al. Mutational profiling of therapy-related myelodysplastic syndromes and acute myeloid leukemia by next generation sequencing, a comparison with de novo diseases. *Leuk Res* 2015;39:348–54.
 38. Qian Z, Fernald AA, Godley LA, Larson RA, Le Beau MM. Expression profiling of CD34+ hematopoietic stem/progenitor cells reveals distinct subtypes of therapy-related acute myeloid leukemia. *Proc Natl Acad Sci U S A* 2002;99:14925–30.
 39. Stoddart A, Nakitandwe J, Chen SC, Downing JR, Le Beau MM. Haploinsufficient loss of multiple 5q genes may fine-tune Wnt signaling in del(5q) therapy-related myeloid neoplasms. *Blood* 2015;126:2899–901.
 40. Haferlach T, Nagata Y, Grossmann V, Okuno Y, Bacher U, Nagae G, et al. Landscape of genetic lesions in 944 patients with myelodysplastic syndromes. *Leukemia* 2014;28:241–7.
 41. Ley TJ, Miller C, Ding L, Raphael BJ, Mungall AJ, Robertson A, et al. Genomic and epigenomic landscapes of adult de novo acute myeloid leukemia. *N Engl J Med* 2013;368:2059–74.

42. Inoue S, Li WY, Tseng A, Beerman I, Elia AJ, Bendall SC, et al. Mutant IDH1 downregulates ATM and alters DNA repair and sensitivity to DNA damage independent of TET2. *Cancer Cell* 2016;30:337–48.
43. Voso MT, Fabiani E, Zang Z, Fianchi L, Falconi G, Padella A, et al. Fanconi anemia gene variants in therapy-related myeloid neoplasms. *Blood Cancer J* 2015;5:e323.
44. Walkley CR, Olsen GH, Dworkin S, Fabb SA, Swann J, McArthur GA, et al. A microenvironment-induced myeloproliferative syndrome caused by retinoic acid receptor gamma deficiency. *Cell* 2007;129:1097–110.
45. Smith LB, Leo MC, Anderson C, Wright TJ, Weymann KB, Wood LJ. The role of IL-1beta and TNF-alpha signaling in the genesis of cancer treatment related symptoms (CTRS): a study using cytokine receptor-deficient mice. *Brain Behav Immun* 2014;38:66–76.
46. Kutyna MM, Wee A, Paton S, Cakouros D, Arthur A, Chhetri R, et al. Aberrant bone marrow microenvironment in therapy related myeloid neoplasm (t-MN). *Blood* 2019;134 (Supplement_1):1694.
47. Schulz E, Valentin A, Ulz P, Beham-Schmid C, Lind K, Rupp V, et al. Germline mutations in the DNA damage response genes BRCA1, BRCA2, BARD1 and TP53 in patients with therapy related myeloid neoplasms. *J Med Genet* 2012;49:422–8.
48. Link DC, Schuettelpelz LG, Shen D, Wang J, Walter MJ, Kulkarni S, et al. Identification of a novel TP53 cancer susceptibility mutation through whole-genome sequencing of a patient with therapy-related AML. *JAMA* 2011;305:1568–76.
49. Churpek JE, Marquez R, Neistadt B, Claussen K, Lee MK, Churpek MM, et al. Inherited mutations in cancer susceptibility genes are common among survivors of breast cancer who develop therapy-related leukemia. *Cancer* 2016;122:304–11.
50. Lepperdinger G. Inflammation and mesenchymal stem cell aging. *Curr Opin Immunol* 2011;23:518–24.
51. von der Heide EK, Neumann M, Vosberg S, James AR, Schroeder MP, Ortiz-Tanchez J, et al. Molecular alterations in bone marrow mesenchymal stromal cells derived from acute myeloid leukemia patients. *Leukemia* 2017;31:1069–78.
52. Bhagat TD, Chen S, Bartenstein M, Barlowe AT, Von Ahrens D, Choudhary GS, et al. Epigenetically aberrant stroma in MDS propagates disease via wnt/beta-catenin activation. *Cancer Res* 2017;77:4846–57.
53. Li H, Durbin R. Fast and accurate short read alignment with burrows-wheeler transform. *Bioinformatics* 2009;25:1754–60.
54. McKenna A, Hanna M, Banks E, Sivachenko A, Cibulskis K, Kernysky A, et al. The genome analysis toolkit: a MapReduce framework for analyzing next-generation DNA sequencing data. *Genome Res* 2010;20:1297–303.
55. Koboldt DC, Zhang Q, Larson DE, Shen D, McLellan MD, Lin L, et al. VarScan 2: somatic mutation and copy number alteration discovery in cancer by exome sequencing. *Genome Res* 2012;22:568–76.
56. Cibulskis K, Lawrence MS, Carter SL, Sivachenko A, Jaffe D, Sougnez C, et al. Sensitive detection of somatic point mutations in impure and heterogeneous cancer samples. *Nat Biotechnol* 2013;31:213–9.
57. Cooper GM, Stone EA, Asimenos G, Green ED, Batzoglou S, Sidow A. Distribution and intensity of constraint in mammalian genomic sequence. *Genome Res* 2005;15:901–13.
58. An N, Khan S, Imgruet MK, Gurbuxani SK, Konecki SN, Burgess MR, et al. Gene dosage effect of CUX1 in a murine model disrupts HSC homeostasis and controls the severity and mortality of MDS. *Blood* 2018;131:2682–97.
59. Stoddart A, Qian Z, Fernald AA, Bergerson RJ, Wang J, Karrison T, et al. Retroviral insertional mutagenesis identifies the del(5q) genes, CXXC5, TIFAB and ETF1, as well as the Wnt pathway, as potential targets in del(5q) myeloid neoplasms. *Haematologica* 2016;101:e232–6.